Supplementary information

Highly Sensitive Detection of *Salmonella Typhimurium* via Gold and Magnetic Nanoparticle-Mediated Sandwich Hybridization Coupled with ICP-MS

Yujie Zhou[a], Zhihui Tang[b], Lei Li[a], Yuzuo Chen[b], Yuanyuan Xu[a], Renjie Liu[b], Yanrong Zhang[b], Xiaoyan Liu[c], Wenjuan Yang[d], Baoning Wang[b], Jieyu Zhang[a,*], Qing Jiang[a*], Yunbing Wang[a,]

[a]National Engineering Research Center for Biomaterials, Sichuan University, Chengdu, Sichuan, 610065, China

[b]West China School of Basic Medical Sciences and Forensic Medicine, Sichuan University, Chengdu, Sichuan, 610041, China

[c]Department of Orthopedic Surgery, West China Hospital, Sichuan University/West China School of Nursing, Chengdu, Sichuan, 610041, China

[d]Department of Gastroenterology, West China Hospital, Sichuan University, Chengdu, Sichuan, 610041, China

*Corresponding author. 29 Wangjiang Road, Chengdu, China, 610065

Tel: +86 028 85410537; Fax: +86 028 85410246

E-mail addresses: jieyu@scu.edu.cn; jiangq@scu.edu.cn

Supplementary methods

1. Determination of grafting density of capture probes on the epoxy-functionalized MNPs

The average diameter of the MNPs was 64 ± 12 nm (Fig. 2b). Despite their clustered morphology, these MNPs were approximated as spheres to calculate the average volume of individual MNP (V_{MNP}).

$$V_{MNP}=\frac{4}{3}\pi(\frac{d}{2})^3=1.37\times10^{-22}\ m^3$$

The density (ρ) of the clustered MNPs was reported to be 3.32 g·cm^{-3},[1] the average mass of an individual MNP was determined as:

$$m_{MNP}=V_{MNP}\times\rho=4.55\times10^{-19}\ kg$$

Considering the silanization layer on the epoxy-functionalized MNPs was very thin (Fig. S9), and the density of GPTMS (1.07 g·mL^{-1}) is much lower than that of the MNPs, the epoxy-functionalization was presumed to have a negligible effect on the overall mass. Therefore, the average mass of an individual epoxy-functionalized MNP was approximated to remain at 4.55 × 10^{-19} kg.

For the capture probe grafting, 0.39 mg of the epoxy-functionalized MNPs was added in each assay. Accordingly, the total number of the epoxy-functionalized MNPs ($A_{\text{epoxy-functionalized MNPs}}$) present in each grafting reaction assay was calculated as:

$$A_{\text{epoxy-functionalized MNPs}}=\frac{0.39\ mg}{m_{MNP}}=8.57\times10^{11}$$

To optimize the process of grafting the capture probes onto the epoxy-functionalized MNPs, 480 μL (V_1) of a capture probe solution at different concentrations (C_{input}) was input into each grafting assay. The total volume of the grafting reaction (V_{total}) was 680 μL. After conjugation, the concentration of the ungrafted capture probes in the mixture was $C_{ungrafted}$. The mass of capture probes grafted onto the epoxy-functionalized MNPs was:

$$m_{grafted}=C_{input}\times V_1-C_{ungrafted}\times V_{total}$$

The molecular weight (M_w) of the capture probes was 6410.3 g·moL^{-1}, thereby the amount of substance of the capture probes grafted onto the epoxy-functionalized MNPs ($n_{capture\ probe}$) was:

$$n_{capture\ probe}=\frac{m_{grafted}}{M_w \text{ of capture probes}}$$

Thus, the total number of the capture probes grafted onto the epoxy-functionalized MNPs ($A_{capture\ probe}$) was:

$$A_{capture\ probe}=n_{capture\ probe}\times 6.02\times 10^{23}$$

Finally, the grafting density of the capture probes on each epoxy-functionalized MNP ($P_{capture\ probe}$) was determined by calculating the number of capture probes grafted per MNP:

$$P_{capture\ probe}=\frac{A_{capture\ probe}}{A_{epoxy\text{-}functionalized\ MNP}}$$

2. Determination of grafting density of report probes on the AuNPs

The average diameter of the AuNPs was measured to be 88 ± 12 nm (Fig. 4a). As illustrated below, despite their popcorn shape, these AuNPs were approximated as

spheres for calculating the average volume of an individual AuNP (V_{AuNP}).

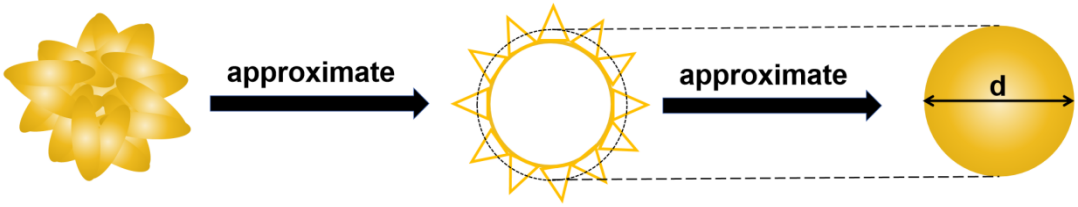

$$V_{AuNP}=\frac{4}{3}\pi(\frac{d}{2})^3=3.57\times10^{-22}\ m^3$$

The specific surface area (α) of an individual spherical AuNP with the same particle size (88 nm) was:

$$\alpha_{spherical\ AuNP}=\frac{4\pi R^2}{\frac{4}{3}\pi R^3}=3.53\ m^2\cdot g^{-1}$$

The density (ρ) of Au is 19.3 $g\cdot cm^{-3}$,[2] the average mass of an individual AuNP was:

$$m_{AuNP}=V_{AuNP}\times\rho=6.89\times10^{-18}\ kg$$

For the report probe grafting, 0.74 mg of the AuNPs was added in each assay. Accordingly, the total number of the AuNPs (A_{AuNPs}) present in the grafting reaction assay was calculated as:

$$A_{AuNPs}=\frac{0.74\ mg}{m_{AuNPs}}=1.07\times10^{11}$$

To optimize the process of grafting the reporter probes onto the AuNPs, 480 μL (V_1) of a report probe solution at different concentrations (C_{input}) was added in each assay. The total volume of the grafting reaction (V_{total}) was 680 μL. After conjugation, the concentration of the ungrafted report probes in the mixture was $C_{ungrafted}$. The mass of report probes grafted onto the AuNPs was:

$$m_{grafted}=C_{input}\times V_1-C_{ungrafted}\times V_{total}$$

The molecular weight (M_w) of the report probes was 6015.0 $g\cdot moL^{-1}$, thereby the amount of substance of the report probes grafted onto the AuNPs ($n_{report\ probe}$) was:

$$n_{\text{report probe}}=\frac{m_{\text{grafted}}}{\text{M}_\text{w}\text{ of report probes}}$$

Therefore, the total number of the report probes grafted onto the AuNPs ($A_{\text{capture probe}}$) was:

$$A_{\text{report probe}}=n_{\text{report probe}}\times 6.02\times 10^{23}$$

Finally, the grafting density of the report probes on each AuNP ($P_{\text{report probe}}$) was determined by calculating the number of report probes grafted per AuNP:

$$P_{\text{report probe}}=\frac{A_{\text{report probe}}}{A_{\text{AuNPs}}}$$

3. Determination of capture efficiency of capture probe-grafted MNPs for *Salmonella* DNA

The *Salmonella* genome, which is haploid, comprises approximately 4.9×10^6 base pairs (bp).[3] Therefore, the M_w of the *Salmonella* DNA can be estimated using the following equation:[4]

M_w of the *Salmonella* DNA=(number of nucleotides×607.4)+157.9=2.98×10^9 g·mol^{-1}

The mass of a single copy of *Salmonella* DNA was then calculated as:

$$m\text{ of each copy }\textit{Salmonella}\text{ DNA}=\frac{\text{M}_\text{w}\text{ of }\textit{Salmonella}\text{ DNA}}{6.02\times 10^{23}}=4.95\times 10^{-9}\ \mu\text{g}$$

Thus, the concentration of *Salmonella* DNA solution, measured using a Nanodrop spectrophotometer and reported in ng·μL^{-1}, can be converted into the number of copies per mL (e.g. copies·mL^{-1}).

To optimize the capture efficiency of the capture probe-grafted MNPs for *Salmonella* DNA, 10 μL of a 10^{11} copies·mL^{-1} *Salmonella* DNA solution (equivalent to 495 ng *Salmonella* DNA) was hybridized with different amounts of the epoxy-

functionalized MNPs over varying durations. Considering the total volume of each hybridization assay was 55 μL and the post-hybridization concentration of the residual *Salmonella* DNA solution was $C_{\text{unhybridized}}$, the capture efficiency (η) can be determined as:

$$\eta=(1-\frac{C_{\text{unhybridized}}\times 55\ \mu\text{L}}{495\ \text{ng}})\times 100\%$$

4. Determination of capture efficiency of report probe-grafted AuNPs for *Salmonella* DNA

Similarly, to optimize the capture efficiency of the report probe-grafted AuNPs for *Salmonella* DNA, 495 ng *Salmonella* DNA in 10 μL of TE buffer was hybridized with varying quantities of the report probe-grafted AuNPs over different durations. Given that the total hybridization reaction volume was 55 μL and the post-hybridization concentration of unhybridized *Salmonella* DNA denoted as $C_{\text{unhybridized}}$, the capture efficiency (η) was also calculated as:

$$\eta=(1-\frac{C_{\text{unhybridized}}\times 55\ \mu\text{L}}{495\ \text{ng}})\times 100\%$$

Supplementary tables

Table S1 Operating parameters of ICP-MS analysis.

Operating parameters	Values
RF power	1550 W
Plasma gas (Ar) flow rate	14 $L \cdot min^{-1}$
Nebulizer gas (Ar) flow rate	0.8 $L \cdot min^{-1}$
Auxiliary gas (Ar) flow rate	0.8 $L \cdot min^{-1}$
Scanning mode	Peak hopping
Isotopes	^{197}Au

Table S2 Information of pathogenic bacteria used in anti-interference assay

Bacterial species	Bacterial strains	Bp
H. influenzae	ATCC 9006	1.9 M
S. pneumoniae	ATCC 6303	2.2 M
E. coli	ATCC 3110	5.9 M
BHS	ATCC 19615	1.9 M
CTB	-	361
AHS	ATCC 49619	1.9 M
N. meningitidis	WHOP	2.3 M
S. pyogenes	ATCC 10389	1.9 M
L. acidophilus	ATCC 13651	2.0 M
P. aeruginosa	ATCC 17434	7.3 M

Table S3 Comparative performance analysis of different detection methods for *Salmonella*.

Detection methods	Nanomaterials	Function of nanomaterials	Morphology of nanomaterials	Detection range (CFU·mL^{-1})	LOD (CFU·mL^{-1})	Recovery	RSDs	Assay time	Refs
Plate culture	-	-	-	-	-	-	-	3 - 7 days	5-9

Detection methods	Nanomaterials	Function of nanomaterials	Morphology of nanomaterials	Detection range (CFU·mL^{-1})	LOD (CFU·mL^{-1})	Recovery	RSDs	Assay time	Refs
PCR	Magnetic beads	Capture of *Salmonella*	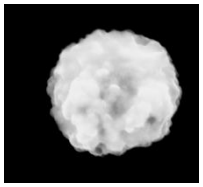 Sphere	6 - 6.4 × 10^4	2	85.9% - 92.1%	-	3 h	[10]
	-	-	-	10^2 - 10^7	2 × 10^2	84.2% - 99.2%	-	24 h	[11]
	-	-	-	-	130	-	-	24 h	[12]

Detection methods	Nanomaterials	Function of nanomaterials	Morphology of nanomaterials	Detection range (CFU·mL^{-1})	LOD (CFU·mL^{-1})	Recovery	RSDs	Assay time	Refs
	Magnetic beads	Capture of *Salmonella*	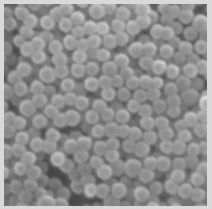 Sphere	-	10^4	-	-	3 - 4 h	[13]
	Magnetic beads	Capture of *Salmonella*	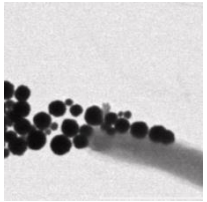 Sphere	-	10^2	-	-	7 h	[14]
	AuNPs	Capture of *Salmonella* DNA	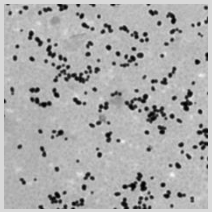 Sphere	-	10 pg·μL^{-1}	-	-	> 55 min	[15]

Detection methods	Nanomaterials	Function of nanomaterials	Morphology of nanomaterials	Detection range (CFU·mL^{-1})	LOD (CFU·mL^{-1})	Recovery	RSDs	Assay time	Refs
Isothermal amplification techniques	-	-	-	2.1×10^2 - 2.1×10^3	2.1×10^1	-	-	50 min	[16]
	-	-	-	-	1.2 - 12 CFU/reaction	-	-	35 min	[17]
	-	-	-	-	10^3	-	-	60 min	[18]

Detection methods	Nanomaterials	Function of nanomaterials	Morphology of nanomaterials	Detection range (CFU·mL^{-1})	LOD (CFU·mL^{-1})	Recovery	RSDs	Assay time	Refs
ELISA	AuNPs	Capture of *Salmonella*	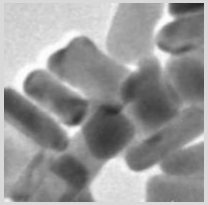 Nanorods	1.21 × 10 - 1.21 × 10^8	1.21 × 10^2	99.2% - 110.7%	-	50 min	19
	MNPs	Capture of *Salmonella*	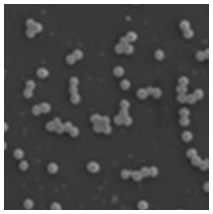 Sphere	-	10 cells·mL^{-1}	90% - 114%	83% - 95%	135 min	20
	Carbon nanotubes	Capture of *Salmonella*	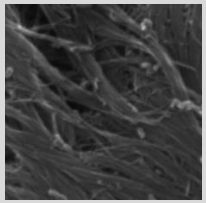 Tubular	-	10^3	-	-	3 h	21

Detection methods	Nanomaterials	Function of nanomaterials	Morphology of nanomaterials	Detection range (CFU·mL^{-1})	LOD (CFU·mL^{-1})	Recovery	RSDs	Assay time	Refs
	MNPs	Capture of *Salmonella*	-	1.4×10^4 - 5.9×10^5	3.2×10^3	82.7% - 117%	-	4 h	[22]
Electro-chemical biosensors	AuNPs	Labelling of *Salmonella* and amplification of signal	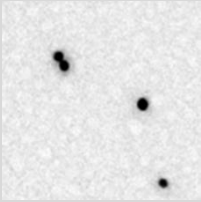 Sphere	10 - 10^6	10	94.2% - 118%	1.4% - 4.5%	1 h	[23]

Detection methods	Nanomaterials	Function of nanomaterials	Morphology of nanomaterials	Detection range (CFU·mL^{-1})	LOD (CFU·mL^{-1})	Recovery	RSDs	Assay time	Refs
	AuNPs and chitosan composite	Electrode materials	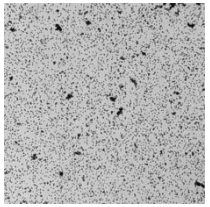 Sphere	10 - 10^5	5	-	-	4 h	[24]
	Reduced graphene oxide and TiO_2 nanoparticles	Electrode materials	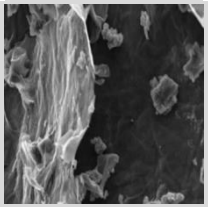 Folded and wrinkled structure	10 - 10^8	10	-	-	1 h	[25]

Detection methods	Nanomaterials	Function of nanomaterials	Morphology of nanomaterials	Detection range (CFU·mL^{-1})	LOD (CFU·mL^{-1})	Recovery	RSDs	Assay time	Refs
	Magnetic beads	Capture of *Salmonella*	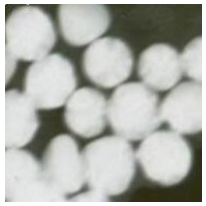 Sphere	10^2 - 10^6	1.04×10^3	-	-	3 h	[26]
Optical biosensors	AuNPs	Colorimetric probes for UV-vis analysis	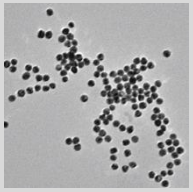 Sphere	25 - 10^5	10	89% - 106.5%	5%	-	[27]
	polyethyleneimine-templated Ag/Cu nanoclusters	Capture of *Salmonella*	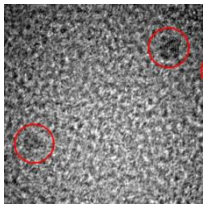 Irregular shape	1.43×10^2 - 1.43×10^7	3.8	83.8% - 103.5%	0.5% - 4.9%	1 h	[28]

Detection methods	Nanomaterials	Function of nanomaterials	Morphology of nanomaterials	Detection range (CFU·mL^{-1})	LOD (CFU·mL^{-1})	Recovery	RSDs	Assay time	Refs
	MNPs	Capture of *Salmonella*	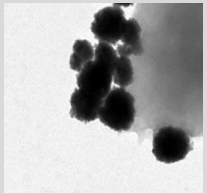 Sphere	10^1 - 10^5	10	80% - 105%	-	2.5 h	29
	AuNPs	Element labels for surface enhanced Raman spectroscopy (SERS) analysis	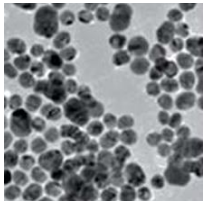 Sphere	10^1 - 10^7	5	-	-	3 h	30
	Fe_3O_4@Si	Capture of *Salmonella*	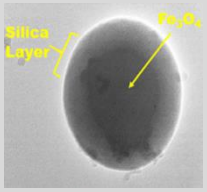 Sphere	1.6×10^1 - 1.6×10^7	4	92.6% - 106.7%	0.7% - 5.5%	-	31

Detection methods	Nanomaterials	Function of nanomaterials	Morphology of nanomaterials	Detection range (CFU·mL^{-1})	LOD (CFU·mL^{-1})	Recovery	RSDs	Assay time	Refs
	AuNPs	Element labels for SERS analysis	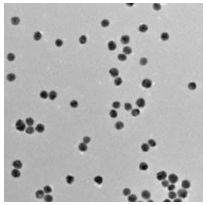 Sphere	27 - 2.7 × 10^5	27	82.9% - 95.1%	-	-	[32]
	MNPs	Capture of *Salmonella*	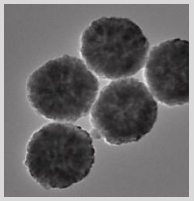 Sphere	10^1 - 10^7	10	97.6% - 100.4%	1.8% - 6.5%	30 min	[33]
	Amorphous carbon nanoparticles	Capture of *Salmonella*	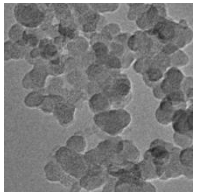 Irregular shape	50 - 10^6	35	83% - 117%	4.7%	-	[34]

Detection methods	Nanomaterials	Function of nanomaterials	Morphology of nanomaterials	Detection range (CFU·mL^{-1})	LOD (CFU·mL^{-1})	Recovery	RSDs	Assay time	Refs
	Au@Platinum nanocatalysts	Labeling *Salmonella*	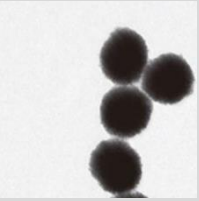 Porous sphere	18 - 1.8 × 10^7	17	88.7% - 110.6%	6% - 8.5%	1 h	[35]
	AuNPs	Capture Salmonella and color	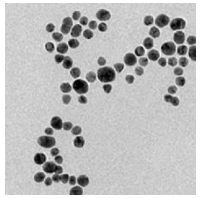 Sphere	7 × 10^1 - 7 × 10^9	23	94.9% - 105.6%	2.4% - 4.9%	2.5 h	[36]
	AuNPs	Element labels for SERS analysis	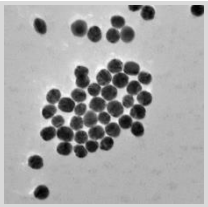 Sphere	10^2 - 10^7	35	94.5% - 105%	-	1 h	[37]

Detection methods	Nanomaterials	Function of nanomaterials	Morphology of nanomaterials	Detection range (CFU·mL^{-1})	LOD (CFU·mL^{-1})	Recovery	RSDs	Assay time	Refs
ICP-MS	AuNPs	Element labels for ICP-MS analysis	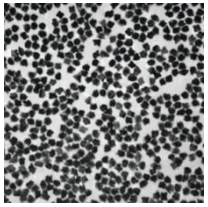 Popcorn-shape	10^2 - 10^5	100	-	-	40 min	[38]
	AuNPs	Element labels for ICP-MS analysis	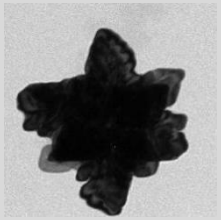 Popcorn-shape	1 - 2.1 × 10^8 (10^1 - 10^{10} copies·mL^{-1})	1	96.8% - 102.8%	0.75% - 1.61%	70 min	This work

Supplementary figures

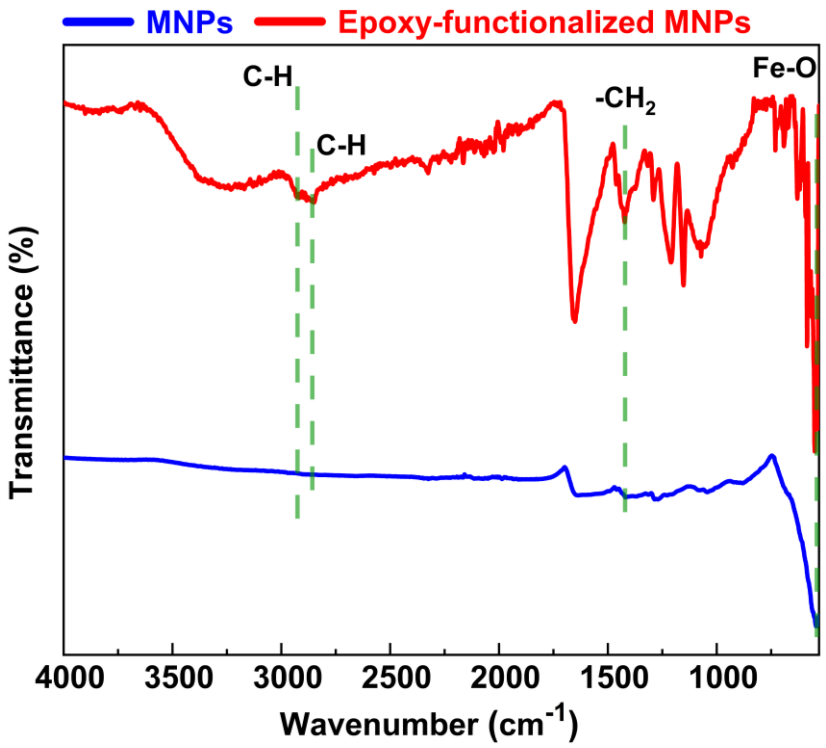

Figure S1. ATR-FTIR spectra of MNPs and epoxy-functionalized MNPs.

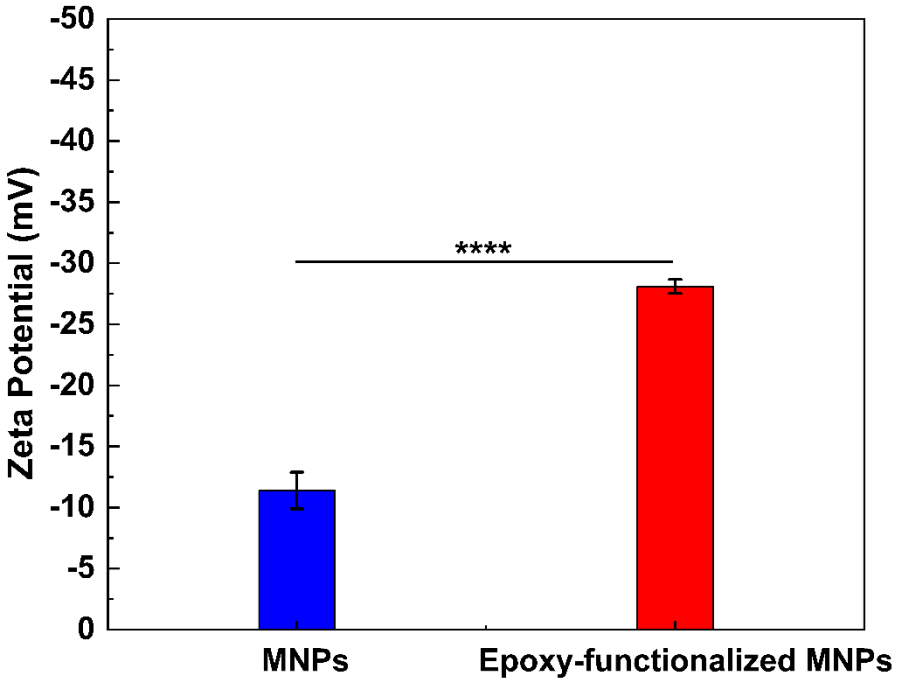

Figure S2. Zeta potential of MNPs and epoxy-functionalized MNPs.

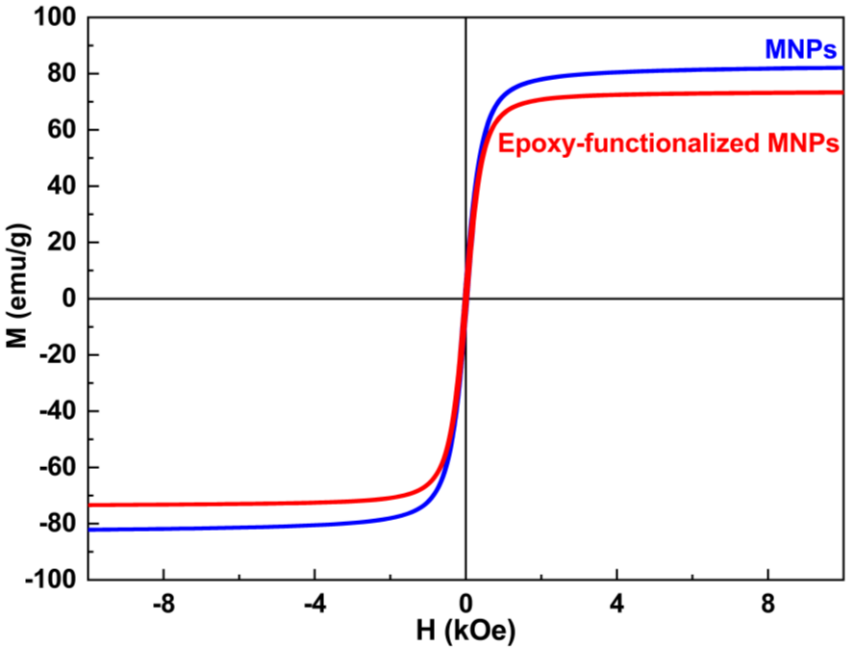

Figure S3. M-H curves of MNPs and epoxy-functionalized MNPs.

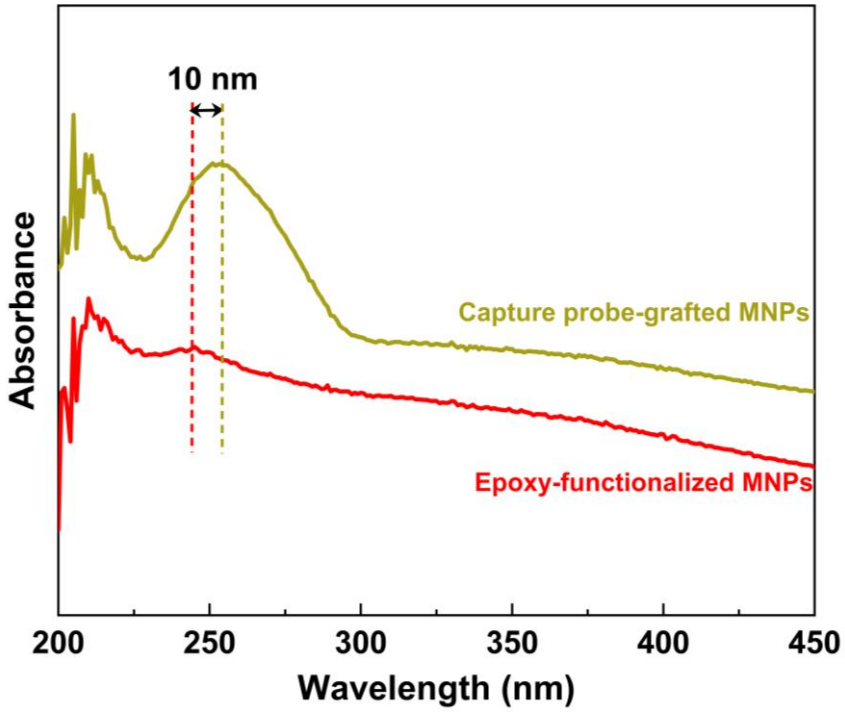

Figure S4. UV-vis spectra of epoxy-functionalized MNPs and capture probe-grafted MNPs.

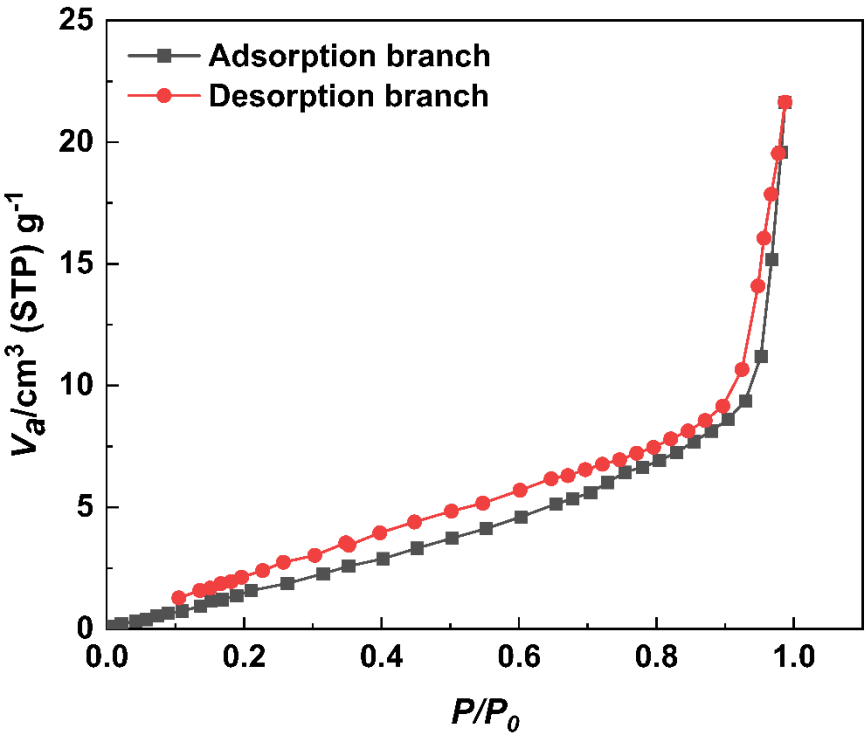

Figure S5. N_2 adsorption-desorption isotherm of AuNPs.

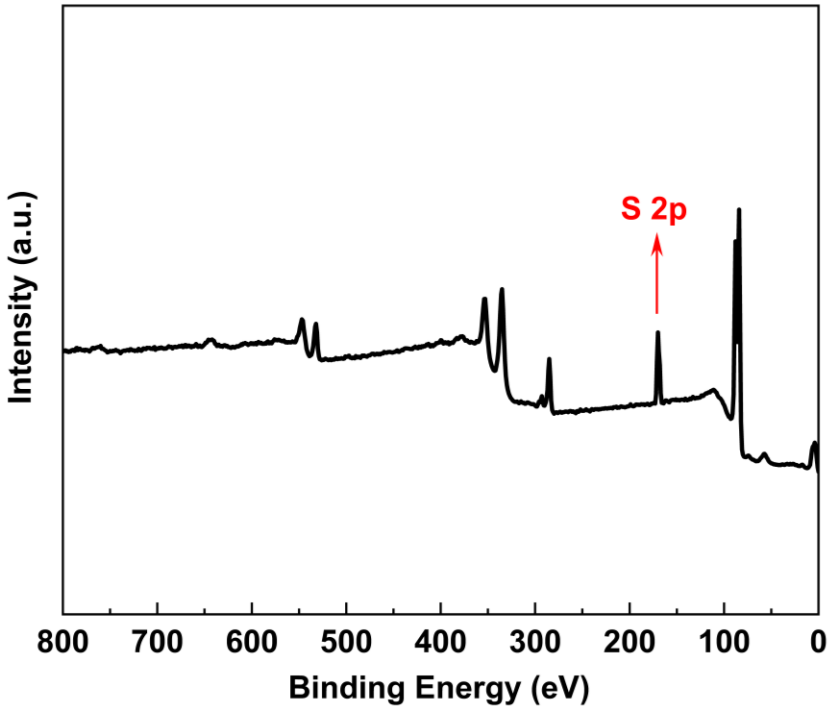

Figure S6. Wide-scan XPS spectrum of report probe-grafted AuNPs.

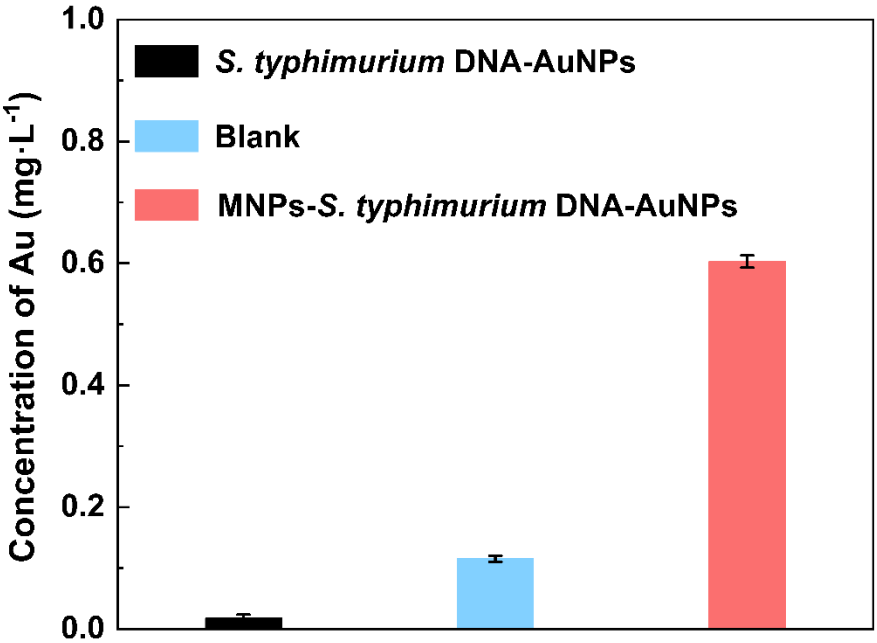

Figure S7. Effect of capture probe-grafted MNPs on isolation of the MNPs-*S. typhimurium* DNA-AuNPs complexes.

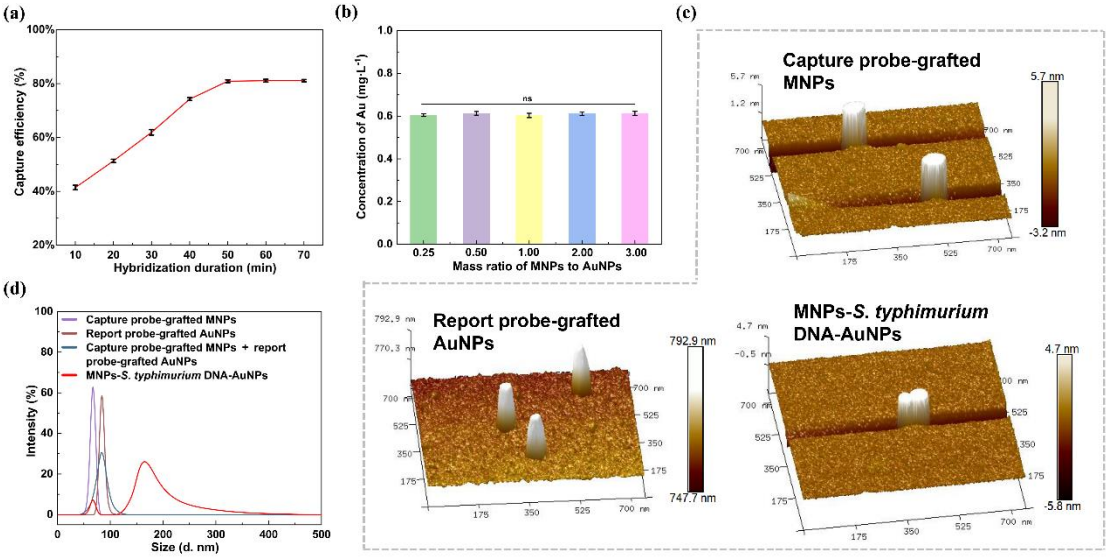

Figure S8. (a) Effect of hybridization duration on the capture efficiency of capture probe-grafted MNPs and report probe-grafted AuNPs on *S. typhimurium* DNA. **(b)** Effect of the mass ratio of capture probe-grafted MNPs to report probe-grafted AuNPs on assay performance. **(c)** AFM images and **(d)** DLS analysis demonstrating the formation of MNPs-*S. typhimurium*-AuNPs complexes.

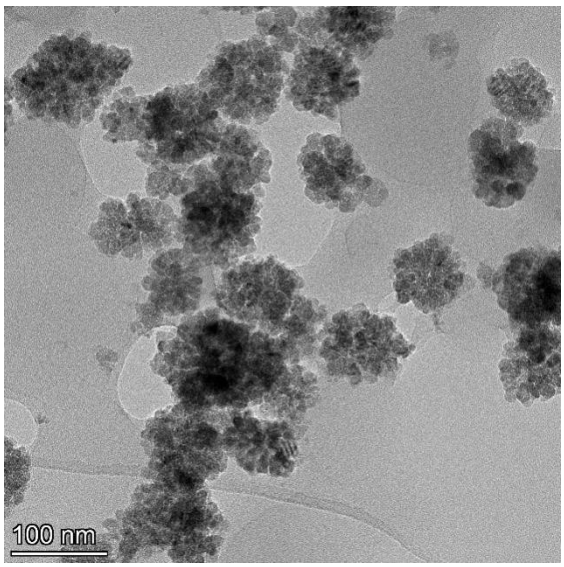

Figure S9. TEM images of the epoxy-functionalized MNPs (68 ± 10 nm).

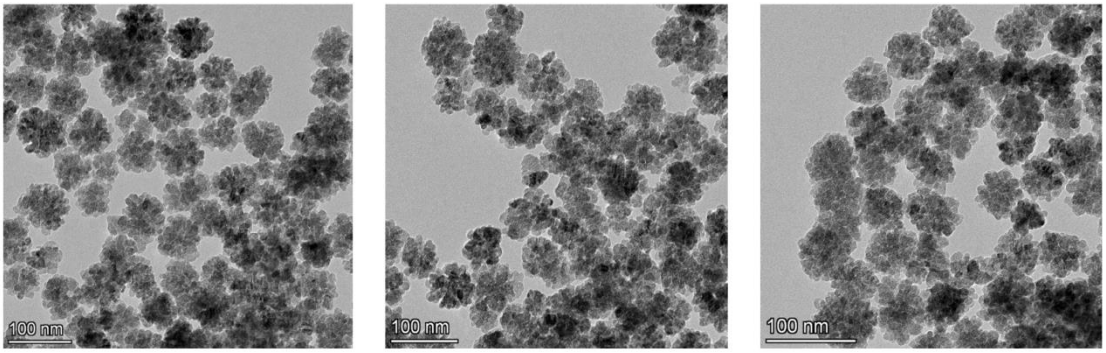

Figure S10. TEM images of three different batches of MNPs synthesized with the V_{EG}/V_{DEG} ratio of 4/16.

References

1 J. Choi, S. Han, K. T. Nam and Y. Seo, *ACS Appl. Nano Mater.*, 2020, **3**, 10931-10940.

2 L. E. Cole, R. D. Ross, J. M. Tilley, T. Vargo-Gogola and R. K. Roeder, *Nanomedicine*, 2015, **10**, 321-341.

3 S. Baker and G. Dougan, *Clin. Infect. Dis.*, 2007, **45**, S29-S33.

4 Y. M. Tseytlin, in *Advanced Mechanical Models of DNA Elasticity*, ed. Y. M. Tseytlin, Academic Press, Boston, 2016, pp.1-37.

5 E. de Boer and R. R. Beumer, *Int. J. Food Microbiol.*, 1999, **50**, 119-130.

6 H. Ayçiçek, H. Aydoğan, A. Küçükkaraaslan, M. Baysallar and A. C. Başustaoğlu, *Food Control*, 2004, **15**, 253-259.

7 P. Arora, A. Sindhu, N. Dilbaghi and A. Chaudhury, *Biosens. Bioelectron.*, 2011, **28**, 1-12.

8 N. Paniel, J. Baudart, A. Hayat and L. Barthelmebs, *Methods*, 2013, **64**, 229-240.

9 R. Ferretti, I. Mannazzu, L. Cocolin, G. Comi and F. Clementi, *Appl. Environ. Microbiol.*, 2001, **67**, 977-978.

10 A. C. Vinayaka, T. A. Ngo, K. Kant, P. Engelsmann, V. P. Dave, M. Shahbazi, A. Wolff and D. D. Bang, *Biosens. Bioelectron.*, 2019, **129**, 224-230.

11 S. Kawasaki, P. M. Fratamico, N. Horikoshi, Y. Okada, K. Takeshita, T. Sameshima and S. Kawamoto, *Foodborne Pathog. Dis.*, 2010, **7**, 549-554.

12 S. Maurischat, B. Baumann, A. Martin and B. Malorny, *Int. J. Food Microbiol.*, 2015, **193**, 8-14.

13 P. Bakthavathsalam, V. K. Rajendran, U. Saran, S. Chatterjee and B. M. Jaffar Ali, *Microchim. Acta*, 2013, **180**, 1241-1248.

14 S. A. Sharief, O. Caliskan-Aydogan and E. C. Alocilja, *Food Control*, 2023, **150**, 109770.

15 J. Du, S. Wu, L. Niu, J. Li, D. Zhao and Y. Bai, *Anal. Methods*, 2020, **12**, 212-217.

16 Y. Shang, Q. Ye, S. Cai, Q. Wu, R. Pang, S. Yang, X. Xiang, C. Wang, F. Zha, Y. Ding, Y. Zhang, J. Wang, X. Sun and J. Zhang, *Lwt*, 2021, **142**, 110999.

17 L. Hu, L. M. Ma, S. Zheng, X. He, T. S. Hammack, E. W. Brown and G. Zhang, *Food Control*, 2018, **88**, 190-197.

18 O. Masashi, O. Yousuke, K. Shuichi, T. Kazuaki, I. Masanari, K. Tadashi and N. Masayuki, *Avian Dis.*, 2009, **53**, 216-221.

19 B. Gao, X. Chen, X. Huang, K. Pei, Y. Xiong, Y. Wu, H. Duan, W. Lai and Y. Xiong, *J. Dairy Sci.*, 2019, **102**, 1997-2007.

20 S. Chattopadhyay, A. Kaur, S. Jain, P. K. Sabharwal and H. Singh, *Anal. Chim. Acta*, 2016, **937**, 127-135.

21 W. Chunglok, D. K. Wuragil, S. Oaew, M. Somasundrum and W. Surareungchai, *Biosens. Bioelectron*, 2011, **26**, 3584-3589.

22 M. Bai, Y. Wang, C. Zhang, Y. Wang, J. Wei, X. Liao, J. Wang, L. Anfossi and Y. Wang, *Food Chem.*, 2023, **424**, 136416.

23 Y. Hou, W. Tang, W. Qi, X. Guo and J. Lin, *Biosens. Bioelectron*, 2020, **157**, 112160.

24 C. Xiang, R. Li, B. Adhikari, Z. She, Y. Li and H. Kraatz, *Talanta*, 2015, **140**, 122-127.

25 S. Muniandy, S. J. Teh, J. N. Appaturi, K. L. Thong, C. W. Lai, F. Ibrahim and B. F. Leo, *Bioelectrochemistry*, 2019, **127**, 136-144.

26 M. Xu, R. Wang and Y. Li, *Talanta*, 2016, **148**, 200-208.
27 N. Duan, B. Xu, S. Wu and Z. Wang, *Anal. Sci.*, 2016, **32**, 431-436.
28 S. Dou, M. Liu, F. Zhang, B. Li, Y. Zhang, F. Li, Y. Guo and X. Sun, *Microchim. Acta*, 2023, **190**, 403.
29 Y. Ding, Z. Li, C. Huang, Y. Zhang, J. Wang and X. Wang, *J. Food Safety*, 2023, **43**, e13091.
30 X. Ma, Y. Liu, N. Zhou, N. Duan, S. Wu and Z. Wang, *Anal. Methods*, 2016, **8**, 8099-8105.
31 S. Sharma, G. Kaur, M. K. Nayak and A. Deep, *Environ. Sci.: Nano*, 2023, **10**, 2473-2488.
32 N. Duan, M. Shen, S. Qi, W. Wang, S. Wu and Z. Wang, *Spectrochim. Acta, Part A*, 2020, **230**, 118103.
33 H. Li, H. Xu, S. Yao, S. Wei, X. Shi, C. Zhao, J. Li and J. Wang, *Talanta*, 2024, **270**, 125505.
34 N. Duan, S. Wu, S. Dai, T. Miao, J. Chen and Z. Wang, *Microchim. Acta*, 2015, **182**, 917-923.
35 L. Zheng, G. Cai, W. Qi, S. Wang, M. Wang and J. Lin, *ACS Sens.*, 2020, **5**, 65-72.
36 F. Zhao, H. Yan, Y. Zheng, Y. Zu, S. Yang, H. Hu, S. Shi, H. Liang and X. Niu, *Food Chem.*, 2023, **426**, 136581.
37 X. Xu, X. Ma, H. Wang and Z. Wang, *Microchim. Acta*, 2018, **185**, 325.
38 Y. Lin and A. T. Hamme II, *J. Mater. Chem. B*, 2015, **3**, 3573-3582.